16th ICAAR LISBOA 2020-2022

16th International Conference on
Alkali-Aggregate Reaction in Concrete
Lisboa | LNEC | Portugal | 31 May - 2 June 2022

http://icaar2020-2022.lnec.pt

Comparison of alkali-silica reaction in low molarity alkali-activated versus Portland-based binary concrete blends

Chloé Monin [(1)], Leah Kristufek [(2)], Diego Jesus de Souza [(3)], Agnes Bezerra [(4)], Leandro Sanchez [(5)], Nicole Hasparyk [(6)]

(1) University of Ottawa, Ottawa, Canada, cmoni019@uottawa.ca

(2) University of Ottawa, Ottawa, Canada, lkris104@uottawa.ca

(3) University of Ottawa, Ottawa, Canada, dsouz025@uottawa.ca

(4) University of Ottawa, Ottawa, Canada, abeze037@uottawa.ca

(5) University of Ottawa, Ottawa, Canada, Leandro.Sanchez@uottawa.ca

(6) Eletrobas Furnas, Goiânia, nicole@furnas.com.br

Abstract

The constant effort to develop sustainable and durable alternatives to Portland cement (PC) concrete has been a major drive for research on alkali-activated concrete (AAC). Although AACs are known for their high chemical resistance, their potential for deleterious induced expansion and deterioration caused by alkali-silica reaction (ASR) remains unclear. This research aims to investigate ASR physiochemical development and its impact on the overall damage of low molarity alkali-activated concrete blends made of conventional supplementary cementitious materials (SCMs), namely fly ash (FA) and slag (SG). Therefore, PC-based (i.e., pure PC, 70%PC-30%FA, and 50%PC-50%SG) and alkali-activated (i.e., 80%FA-20%SG and 80%SG-20%FA) concrete specimens were manufactured and stored in conditions enabling ASR-induced development as per ASTM C 1293 (i.e., 38°C and 100% R.H.) and monitored over time. After four months of exposure, microscopic (i.e., Damage Rating Index – DRI) and macroscopic (i.e., Stiffness Damage Test – SDT and compressive strength) test procedures were conducted and revealed that while ASR did develop in all mixes, the extent of microscopic damage and loss in mechanical properties was substantially lower in SCMs-containing PC and AAC mixtures than in PC mixtures. In contrast with PC mixes, the causes of expansion and mass gain in AAC mixes were shown to be multifactorial.

***Keywords**: Alkali-activated concretes, alkali-silica reaction, low molarity, macroscopic analysis, supplementary cementing materials*

1. INTRODUCTION

Concrete is a widely used material for critical infrastructure worldwide: over 10 billion tons of concrete are produced annually [1]. In addition, its demand is anticipated to grow up to approximately 18 billion tons annually by 2050 [2]. However, the construction industry is facing crucial challenges to find cost-effective strategies to reduce the carbon-footprint and embodied energy associated with the production and use of concrete and its ingredients [3]. Portland cement (PC) is by far the most important ingredient of concrete and also the main responsible for its carbon-footprint, accounting for about 7% of the annual man-made CO_2 emissions [4]. As a result, the interest of the scientific community for eco-friendly alternatives to PC is growing exponentially, with some of the most promising alternatives being alkali-activated concrete (AAC) [5–7]. Literature findings suggest that AAC provide materials with high mechanical properties [8, 9] and durability [10–12]. These materials are synthesized by reacting amorphous aluminosilicate precursors (i.e., minerals or waste materials) with a highly alkaline activator solution. Overall, alkali-activated binder systems can be divided into three categories based on their calcium content (i.e., geopolymers, intermediate and high calcium AAC) [13]. This distinction is necessary due to the large impact of calcium on the hardened material's gel composition and microstructure, and therefore its resistance against chemical attacks [14–17]. Even though the chemical resistance of AAC mixtures appears very promising [18, 19], the high alkalinity of AAC's pore solution has raised concerns on their susceptibility to alkali-silica reaction (ASR) [20]. Yet, few studies have been published on the subject [20, 21] and contradictory results were obtained [22–25]. Moreover, most of the research was performed on mortars subjected to 80°C and soaked in 1 mol NaOH (i.e., ASTM C1260) [25–27], despite this testing method being criticized for its extremely aggressive environment and short time duration [25, 28–30], thus providing inaccurate results when applied to low calcium AAC

[25, 30–32]. A systematic investigation is thus needed to better understand the mechanism of ASR in the AAC system. This works aims to appraise the early development of ASR in low-molarity alkali-activated concrete of intermediate and high calcium content incorporating highly reactive coarse aggregates in comparison with SCMs-containing PC based concrete. Furthermore, because more studies are needed to understand ASR development in low alkali binary AACs and evaluate how it differentiates from ASR development in SCMs-containing PC, a dual and multi-scale approach to the investigation of ASR has been adopted to improve the understanding of the resistance of both alkali-activated and Portland binder systems.

1.1 ASR development in alkali-activated materials

ASR is one of the most harmful distress mechanisms affecting the durability and serviceability of concrete infrastructure. ASR is conventionally defined as a chemical reaction between alkalis (Na+, K+ and OH−) dissolved in concrete's pore solution, and some reactive mineral phases containing reactive silica forms present in the aggregates [33–37]. ASR generates a gel that swells in the presence of water, causing volumetric expansion and distress in the affected material [36]. The degree and features of ASR damage depends upon the type (i.e., fine or coarse aggregate) and reactivity of the aggregates used, the amount of alkalis in the concrete, as well as the temperature and relative humidity of the environment [35, 36, 38–42]. This section will focus on the development of ASR in AAC.

Literature shows that two competitive factors must be considered for the study of ASR; the first being related to their very high alkali content, and the second being that most precursors used in alkali-activated concrete are supplementary cementitious materials (SCMs) with the potential to mitigate ASR in PC concrete. Regarding alkali content, although many studies have found that a higher alkali dosage leads to an increase in pore solution alkalinity and ASR gel amounts [23, 29, 43, 44], the relationship between the two remains a subject of debate. Indeed, greater pore solution alkalinity appears to impact ASR in seemingly conflicting ways. While the additional alkalis may worsen ASR, the higher alkali content has also been reported to increase precursor dissolution [45]. This can lead to elevated aluminium content in the pore solution, which results in a decreasing silica dissolution rate [46]. Additionally, more fully reacted binders have a greater alkali binding capacity, therefore their initially high pore solution alkalinity may decrease over time. These two mechanisms may explain the results obtained by Shi *et al.* and Yang *et al.* [46, 47] who reported lesser ASR gel amounts with an increase in alkali dosage. In particular, it appears that in pure sodium hydroxide activated AACs, the expansion increases as the molarity decreases [46]. Furthermore, the discrepancy in several authors' findings of the impact of alkali content on ASR may have found some explanation by the investigation of multiple parameters (i.e., silicate modulus, alkali dosage and alkali cation) [21], as in the recent study by Tänzer *et al.* [23]. There remains a need to further investigate ASR resistance of low alkali (2M) sodium hydroxide AACs.

As for the choice of aluminosilicate precursors and their impact on preventing ASR, the large differences in their chemistry can partially account for the expansion disparities in AACs. Three main categories of behavior were defined from the literature [20, 21, 48]: (1) AAC is unlikely to suffer from deleterious ASR, (2) AAC has a similar resistance to ASR as PC concrete's, (3) AAC exhibits poorer resistance to ASR than PC concrete. The first case mostly apply to low-calcium AACs [22, 32, 43, 49, 50], although it has been observed sporadically in high-calcium AACs [51]. The key role of calcium in the formation of expansive ASR was investigated in many studies and could explain the limited amounts and innocuous nature of ASR gels in pure fly-ash and metakaolin AACs [27, 52]. On the other hand, alkali-activated slag concrete and other high calcium AACs are predominantly found in the second category [24, 30, 50, 53] and, to a smaller extent, in the third one [28, 32]. The high alkali binding and low calcium availability of these binders may explain why most slag-based concrete fall into the second category [54, 55]. However, the reason why certain high calcium AACs are in the third category remains unclear. Moreover, the behavior of binary AACs comprising low and high calcium precursors is not well understood. From the very few studies published on the subject [22, 50, 56], it is not yet clear how binary AACs resist to ASR.

2. SCOPE OF WORK

The long-term resistance of AAC mixtures and of SCMs-containing PC concrete mixtures to ASR remains an active field of study. The aim of this work is to shed light on the early development of ASR

in low-molarity AACs of intermediate and high calcium content (i.e., respectively 80% fly ash-20% slag, and 20% fly ash-80% slag), as well as in Portland-based concrete containing either 30% fly ash or 50% slag. Concrete specimens made with highly reactive coarse aggregates (crushed Greywacke) were stored for four months in an environment enabling ASR-induced development as per ASTM C 1293. Several of their macroscopic and microscopic properties were monitored over time to appraise how their properties were impacted by or were susceptible to impact ASR development. The influence of ASR on mechanical properties was assessed through compressive strength and stiffness damage testing. The extent of microscopic damage induced by ASR was also evaluated. Additionally, the length and mass of the samples were monitored monthly.

3. MATERIALS AND METHODS

3.1 Materials and concrete mix design

Two alkali-activated and three PC concrete mixes were designed following the guidelines of ASTM C1293 except for the size of specimens and the alkali boosting in AACs [57]. All concrete mixes were prepared with a non-reactive fine aggregate (manufactured sand) and with a highly reactive coarse aggregate (crushed Greywacke). The volume of reactive coarse aggregate and the water-to-cement ratio (0.45) were fixed in all mixtures. The mix-design of the concrete mixtures can be found in Table 3-1. The alkali-activated binder of the two families comprises respectively 80% of fly ash and 20% ground blast furnace slag (AAC-FA), and 20% fly ash and 80% ground blast furnace slag (AAC-SG). The activator solution is made of 2 mole sodium hydroxide solution, which brought the NaO_2 content to 5.23% for the AAC-FA mix, and to 3.85% for the AAC-SG mix. As these values are beyond the 1.25% NaO_2 content prescribed by ASTM C1293, no additional alkalis were incorporated. In the PC mixtures, a fraction of cement was replaced with fly ash (PC-FA) or slag (PC-SG). To allow ASR development in these mixes, the percentage of SCMs added was chosen to be slightly below the necessary amount to completely mitigate ASR in the short term. An ordinary Portland cement concrete (OPC) was also manufactured to serve as control. Sodium hydroxide was added to bring the total NaO_2 content to 1.25% in all PC concrete batches. The chemical composition of binder constituents can be found in Table 3-2.

Table 3-1: Mix-design of the alkali-activated and Portland cement mixtures

		AAC-FA	AAC-SG	PC-FA	PC-SG	OPC
Activator (kg/m³)	Water	189				
	Dry NaOH	15	15	-	-	-
Binder (kg/m³)	SG	84	336	-	210	-
	FA	336	84	126	-	-
	PC	0	0	294	210	420
Aggregates (kg/m³)	Coarse	938				
	Fine	694	800	776	822	836

Table 3-2: Chemical composition of the binder's components

Composition (%)	SiO_2	Al_2O_3	CaO	Fe_2O_3	SO_3	MgO	Na_2O	LOI
SG	36.64	11.14	37.32	0.4	0.37	12.15	0.63	0.49
FA	56.31	23.27	10.29	3.57	0.19	1.07	3.17	0.98
PC	20.1	5.03	61.93	3.8	3.38	2.42	0.91	2.1

3.2 Manufacture of the concrete specimens

A total of 45 concrete cylinders of 200 mm of length and 100 mm of diameter were cast per mix instead of the concrete prisms recommended by the ASTM C1293 standard. After 24 hours of moist curing, samples were demolded, and small holes were drilled. Studs were inserted with a fast-setting cement. The samples were moist cured again for 48 hours until the zeroth measurements of length and mass were made. The cylinders were then placed in sealed buckets in 100% relative humidity conditions and stored in a 38°C chamber, except for a few that were wrapped and kept at 12°C to prevent ASR development and be used as sound specimens. The buckets were removed monthly from the chamber, and length and mass measurements were conducted on cylinders once they reached room temperature.

After four months, a few samples chosen for macroscopic and microscopic testing were removed from the ASR-inducing storage conditions and were wrapped and kept in a 12°C chamber to stop ASR development until testing. At least 48 hours before testing, the samples were removed from the chamber and put at 100% relative humidity at room temperature, following the procedure for testing cores from concrete structures (CSA A23.2-14C) [58]. The cylinders' studs were then removed, and the samples were mechanically ground to achieve a flat surface on both ends.

3.3 Assessment of ASR development

3.3.1 Macroscopic testing

The first compressive strength testing was performed on three sound cylinders after a 47-day curing period according to the maturity concept specified in ASTM C 1074 [59]. The second compressive strength measurements were carried out on three cylinders kept in ASR-inducing conditions and used for stiffness damage testing (SDT), with the aim of verifying the compressive strength loss of concrete as a function of AAR development. This procedure was adopted and considered valid after Sanchez *et al.* [35, 60] confirmed the SDT's non-destructiveness. Regarding the SDT procedure, the same approach as proposed in Sanchez *et al.* [35, 41, 61] was chosen, i.e. using a loading level corresponding to 40% of the 28-day compressive strength of the sound samples, and five cycles of loading/unloading at a controlled loading rate of 0.10 MPa/s.

3.3.2 Microscopic testing

The damage rating index (DRI), a semi-petrographic method, was used to evaluate the extent and patterns of cracking in both sound samples and samples kept in ASR-inducing conditions, according to the method described by Sanchez *et al.* [35, 60]. The DRI final number presented in this work is the normalized 100 cm^2 value obtained over semi-polished concrete specimens. Even though alkali-activated binders are "cement-free" materials, the original taxonomy of petrographic features as presented in Table 3-3 is followed for all mixtures to facilitate the comparison between AAC and PC batches.

Table 3-3 Weighing factor per petrographic feature for the DRI method [60]

Petrographic features		Weighing factors
Crack in coarse aggregate	CCA	0.25
Opened crack in coarse aggregate	OCA	2
Crack with reaction product in coarse aggregate	OCAG	2
Coarse aggregate debonded	CAD	3
Crack in cement paste	CCP	3
Crack with reaction product in cement paste	CCPG	3
Disaggregate/corroded aggregate particle	DAP	2

4. RESULTS AND DISCUSSION

4.1 ASR kinetics

In this section, ASR expansion kinetics and amplitude results are presented for all five mixtures. Figure 4-1a shows the average expansion values of each mixture, while Figure 4-1b shows the mass variation over time. A wide range of expansion kinetics and amplitudes were obtained as a function of the mixtures tested. In general, the control mixture (OPC) displayed faster ASR kinetics and higher expansion amplitudes (i.e., 0.31% at 130 days) than those incorporating SCMs. The use of SCMs in both alkali-activated and PC systems slowed down ASR kinetics. Moreover, it is worth noticing that SCMs-containing PC concrete mixtures exhibited 63% expansion decrease compared with AAC mixtures. It is well known in the literature that SCMs are a powerful preventive measure against ASR development. Overall, SCMs can enhance concrete microstructure, impacting the mobility of ions and possibly slowing the reaction rate [62–64]. Likewise, these materials are able to dilute the alkalis available from the clinker and change the properties of ASR reaction products by consuming $Ca(OH)_2$ from the concrete pore solution [33, 64, 65]. Furthermore, the difference in calcium content of the SCMs used in this research

could be a determining factor to account for the differences in expansion development of PC-FA and PC-SG mixes.

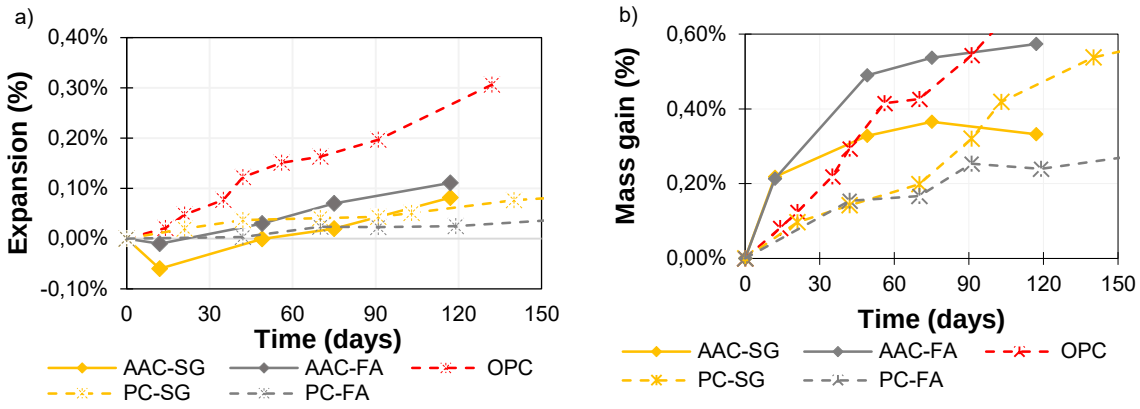

Figure 4-1 a) ASR expansion development over-time, and b) mass gain over-time

Similarly, AAC-SG's and AAC-FA's expansion values demonstrated comparable behavior, yet AAC-SG displayed lower values than AAC-FA during the testing period. The "slag-rich" alkali-activated samples (AAC-SG) developed considerable shrinkage within the first weeks of testing which is in agreement with past studies [66, 67]. In comparison with the fly ash- and slag-containing PC samples, and despite initial shrinkage, both alkali-activated samples exhibited faster ASR kinetics rates. This difference in behavior may be partially explained by the higher alkali content of AAC samples. However, the expansion amplitudes of the AAC mixtures studied in this research are higher than most values reported in the literature [50, 56], so the alkali content is unlikely to be the only influencing factor. It is worth speculating that two main factors could be responsible for the behavior of AAC samples: the high reactivity of the aggregates and the low molarity of the sodium hydroxide activator solution. ASR resistance of AAC to such highly reactivity aggregate has rarely been reported in the literature [32, 56], and is still largely unknown. The low molarity NaOH solution might also have worsened the vulnerability of the AAC mixes to ASR. As discussed previously, the absence of sodium silicate in the activator and low alkali content could impair precursors' dissolution and limit the reaction extent. Consequently, lesser amounts of calcium aluminosilicate hydrate (C-A-S-H) and sodium aluminosilicate gel (N-A-S-(H)) would form in the AAC blends. In other words, we may hypothesize that the relative proportion of alkalis in pore solution may increase as a result of lesser reacted phases.

The mass variation of the specimens over time was also monitored to correlate microstructure and ASR development with the expansion. Figure 4-1b illustrates that mass variation does not always correlate with length variations. Overall, there is significant mass gain in all mixes. Since cylinders are stored at 100% of relative humidity, mass increase is attributable notably to moisture absorption. This may be associated with changes in the pore system capacity during hydration, integration into hydrate products and formation of detrimental products like ASR gel. While both expansion and mass values appear to increase steadily for PC specimens, mass measurements fluctuate in AAC and SCMs-containing specimens. The mass of the PC-SG specimens starts increasing significantly faster than PC-FA specimens' mass after two months. Since the difference in expansion values between the two SCMs-containing PC mixtures also increased at the same time, the cause of the sudden mass gain of PC-SG samples could be correlated with more ASR product formation. As for the alkali-activated samples, both mixtures followed similar trends: the mass gain rate was particularly high during the first month, followed by more stable values from the second month onward. Even though the control OPC samples exhibited much larger expansion, their mass gain was smaller than that of AAC-FA until the third month of monitoring, and that of AAC-SG until the second month of monitoring. As explained by Shi *et al.* [46], the ongoing hydration process of alkali-activated materials over the first months may also contribute to the mass increase. Thus, the slower development of microstructure in AACs could partially explain the difference in mass variation between the alkali-activated and PC binder systems. The higher sorptivity of AAC could also have led to greater water uptake by these samples and thus larger mass gain [68]. Moreover, the stabilization of the mass of alkali-activated samples after three months while length measurements were still increasing seems to indicate that the early mass gain experienced by AAC was mainly caused by hydration and water uptake. Differences in mass increase between AAC mixtures may

be partially accounted for by the difference in expansion values, but it appears likely that the kinetics of reaction in low versus high calcium AAC could have played a larger role. Another factor to be considered is the lower porosity of mixes with fly ash, which would be expected to limit moisture loss. The evolution of mechanical properties will be discussed in the following section to further investigate the causes of mass and length variations.

4.2 Macroscopic testing

The results of compressive strength and SDT testing are reported for both AAC and PC mixes in Figure 4-2. From these results, there is a very significant difference between the mechanical properties of AAC and PC binders over the testing period. The performance of OPC control samples was initially satisfactory but largely decreased after four months of exposure to ASR-inducing conditions. Strength and modulus of elasticity losses of 22% and 48% respectively were observed in the OPC mixture, which correlates to its high expansion. In comparison, the compressive strength remained stable in both fly ash and slag PC mixtures (increase < 5%). Although fly ash and slag Portland cement mixes showed signs of expansion after four months, their expansion level remained below 0.05%. The absence of impact on mechanical properties is thus in agreement with the qualitative AAR damage model proposed by Sanchez *et al.* [40]. According to the model, the cracks formed during the early stages of ASR are mostly confined to the aggregate particles, with very few cracks in the cement matrix. The concrete strength is thus largely unaffected by ASR development at this stage. Pozzolanic reactions of the SCMs cause a small increase in the compressive strength at four months. However, the modulus of elasticity of those mixtures shows a small decrease during this same period, which may indicate the beginning of damage in SCMs-containing samples.

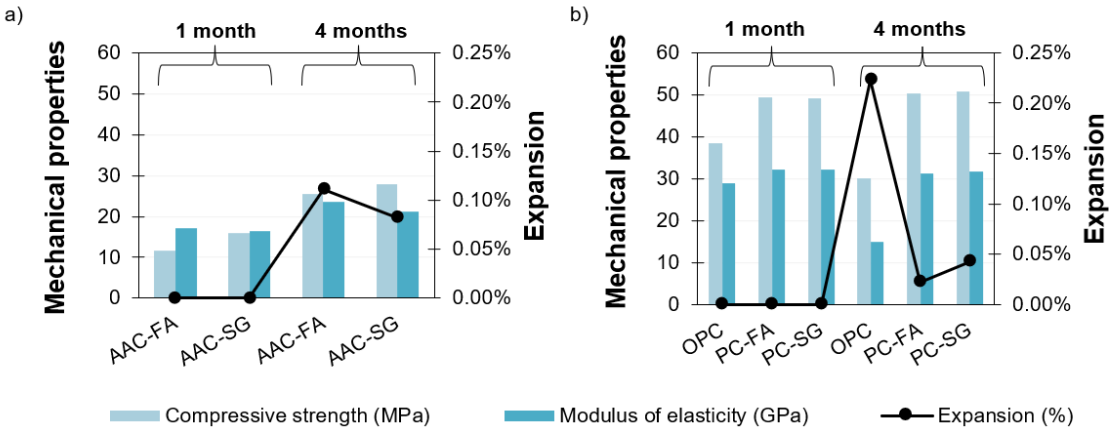

Figure 4-2 Compressive strength and modulus of elasticity of the (a) alkali-activated and (b) Portland-based samples at 28 days and after 4 months

Conversely, AAC samples displayed radically different behaviors for both the evolution of compressive strength and modulus of elasticity. Even though both high and low calcium AAC experienced moderate expansion levels, the increase in compressive strength reached 120% and 76% for the AAC-FA and AAC-SG mixes, respectively. As expected, the growth in compressive strength led to higher moduli of elasticity, with increases ranging from nearly 30% to almost 40%. Significant improvements in mechanical properties over the first months after batching are not uncommon for alkali-activated materials. It may explain why in spite of the moderate expansion level reached by the AAC samples, their mechanical properties improved more rapidly than damage could develop. Furthermore, while both AACs gained in strength and modulus of elasticity, the properties of the AAC-FA mix improved more than those of the AAC-SG mix. Since the level of expansion attained by the AAC-FA mix is higher than that of the AAC-SG mix, it appears unlikely that this difference could be caused by a greater extent of damage in AAC-SG samples. Rather, because of the dual influence of calcium and precursors' reactivity on AAC properties' development [69], it is more likely that the difference in mechanical property evolution over the observation period is governed by the proportions of precursors.

The raw values from SDT enabled the calculation of Stiffness Damage Index (SDI) and Plastic Deformation Index (PDI) for the two concrete mixes. These indices indicate the ratio of dissipated energy over total energy during the test. This enables for a more reliable assessment of damage [70],

independently of the type of reactive aggregate or the strength of the concrete [70, 71]. Results from the OPC control samples demonstrated high increases in both the SDI and PDI values at four months, which is consistent with an expansion level of 0.3%. PC-FA had moderate increases in SDI (43%) and PDI (14%), while PC-SG had moderate decreases in SDI (31%) and PDI (18%). This indication of lower damage is consistent with the lower expansion observed in these samples and, in the case of PC-SG, may indicate ongoing hydration causing increased strength. In the AAC samples, significant decreases in SDI and PDI occurred, indicating improved mechanical properties. For both AAC-FA and AAC-SG, the SDI and PDI decreased up to 80% over the testing period. The SDI at four months was higher for PC-SG, suggesting poorer mechanical properties than SG-FA. This is inconsistent with the observed expansion. Again, this difference is thought to be caused by the difference in strength gain between the two AAC families arising from different hydration mechanisms and calcium contents. Finally, the mechanical testing results show that both PC and PC-FA appear to be affected by ASR damage. However, the improvement in mechanical properties of AACs and of PC-SG mixtures raises the need for microscopic analysis to confirm the presence of ASR and the onset of ASR-induced damage in these specimens.

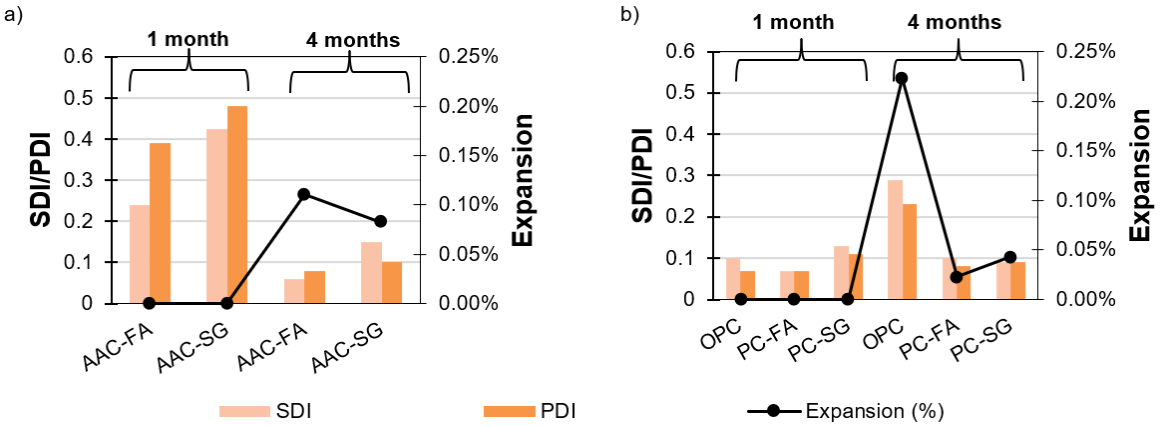

Figure 4-3 SDI and PDI of the (a) alkali-activated and (b) Portland-based samples at 28 days and after 4 months

4.3 Microscopic testing

Using DRI analysis, the features and extent of cracking were evaluated in samples after 4 months of exposure and were compared with cracking in sound samples after a month of curing. After weighting the different crack types, the DRI number of each mixture was evaluated and is illustrated in Figure 4-4. From the results shown in Figure 4-4, it can be observed that the PC mixes had initially very low DRI numbers in comparison with AAC mixes. Furthermore, large counts of open cracks with and without gel in the aggregate, as well as cracks within the cement paste developed in the OPC samples over the course of four months. High amounts of cracks in coarse aggregates (CCA) were also initially present in PC-based samples and appear, most likely, as the result of processing operations or weathering. The number of closed cracks within the aggregates remained constant for the testing period, which seems to indicate that many of those cracks were present in the aggregates prior to batching. These results confirm that the OPC mix was very affected by ASR damage after four months of exposure. Conversely, the SCMs-containing mixes appear much less damaged. Even though both the distribution of cracks and DRI number were initially similar in all PC mixtures, the fly ash- and slag- containing samples only saw a moderate increase of the DRI number, mainly due to greater open cracks in the aggregate (OCA) counts after four months. Interestingly, PC-SG samples exhibited a higher DRI number than PC-FA samples, and in contrast to the fly ash samples, they displayed the onset of open cracks in the aggregate with gel (OCAG). This behavior conflicts with mechanical testing results but accords with the expansion values reported. It is likely that the greater strength gain of PC-SG specimens has prevented mechanical properties loss in the short term. Moreover, this finding highlights the need to perform multi-scale testing when establishing an ASR diagnostic. It appears especially true for ASR detection in AACs given the apparent contradiction in mechanical, versus length and mass measurements results.

In AAC families, the initial DRI numbers were exceptionally high, especially with regards to the cracks in the cement paste (CCP) and OCA cracks. In addition, the interfacial transition zone in both AAC

mixtures appears highly porous at 28 days, especially in the case of AAC-SG, which showed with a high number of macropores, and cracks perpendicular to the aggregates indicating strong signs of shrinkage. These cracks were classified as CCP, which heavily contributed to the high DRI numbers obtained for the two AAC mixtures. Those results are indicative of poor microstructure in the early days of the testing period. This may be explained notably by the large strength gain observed for the AAC samples, which showed that important changes on a microscale were taking place during the first months of testing. Furthermore, the sound (1-month) samples were moist cured at ambient temperature for the first 48 hours and then kept at low temperature (12°C) and humidity until testing to prevent ASR development. To the best knowledge of the authors, the impact of this procedure on the maturity of AAC concrete has not been previously studied, and it remains unclear if it could have negatively impacted the microstructure of the sound (1-month) samples. Furthermore, it is well known that elevated temperatures are beneficial to fly ash-containing AACs [72]. Thus, the 38°C conditions might have increased fly ash dissolution and contributed to the gain in mechanical properties. Indeed, the microstructure of alkali-activated samples at four month appears significantly improved, as shown by the considerable decrease in CCP count. At the same time, a slight increase in OCA and OCAG cracks is noticeable in the AAC-FA samples. Even though this was not observed in the AAC-SG mixture, about 30% of the CCP cracks in AAC-SG samples were “through-aggregate” cracks typical of ASR damage. In contrast, the cracks observed in AAC-FA were not related to the aggregates, which indicates that most were unlikely to result from ASR. From these results, it may be concluded that the extent of ASR damage in AACs was small. This further confirms that ASR development was not the only cause of the expansion observed in the samples. Further studies are needed to better understand the etiology of the expansion and the ASR development at later ages.

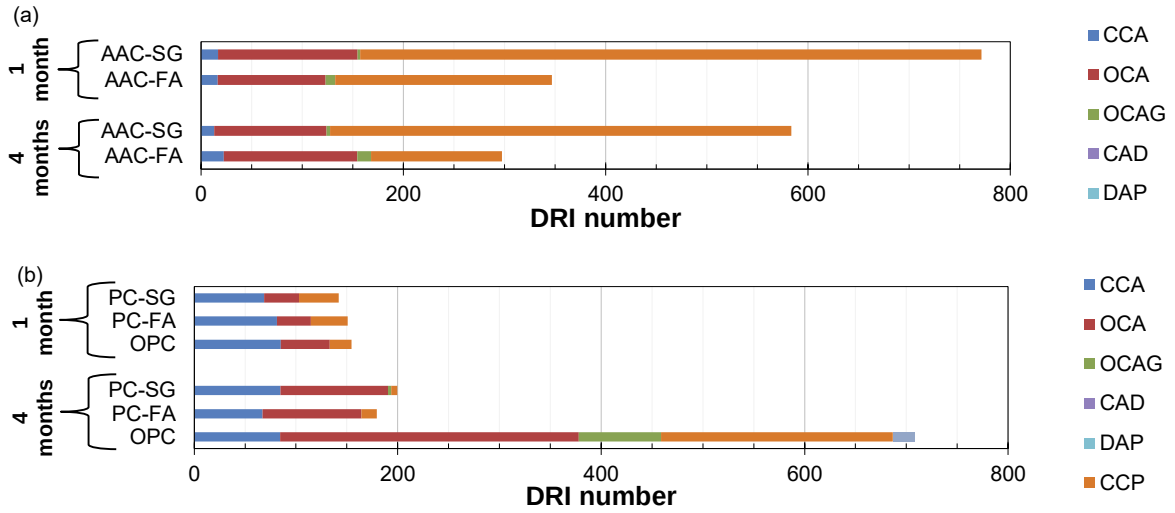

Figure 4-4 DRI number of (a) alkali-activated mixes and (b) Portland-based mixes at 28 days and after 4 months

5. CONCLUSIONS

This study showed the assessment of ASR impact on a macroscopic and microscopic level for alkali-activated and Portland-based concrete mixtures. The following conclusions may be drawn:

- All mixes performed better than the control OPC mixture in the modified ASTM C 1293 using the same reactive coarse aggregate.
- Mechanical behavior captured through SDT using SDI and PDI indices indicate that hydration behavior was substantially different for AAC and PC-based mixes. AAC mixes exhibited poor initial mechanical properties but substantial improvements at 4 months. Assessment of ASR damage using this technique will require calibration to capture the effect of ASR on AAC materials.
- ASR damage features were observed in all samples, but to a much greater extent in OPC samples. Due to porous microstructure in the early stages, the cracking in alkali-activated samples diminished over the testing period. The observation of few ASR distress features in AAC specimens led the authors to believe that the samples have only been slightly affected by

ASR, which is in contradiction with the expansion results. Further work is ongoing to better understand the etiology of expansion and mass gain in AAC.

6. REFERENCES

1. Meyer C (2009) The greening of the concrete industry. Cem Concr Compos. https://doi.org/10.1016/j.cemconcomp.2008.12.010
2. Mehta PK, Monteiro PJM (2014) Concreto Microestrutura, Propriedades e Matérias. In: IBRACON. São Paulo, p 782
3. Worrell E, Price L, Martin N, et al (2001) Carbon dioxide emissions from the global cement industry. Annu Revis Energy Environ 26:303–329
4. Limbachiya M, Bostanci SC, Kew H (2014) Suitability of BS EN 197-1 CEM II and CEM V cement for production of low carbon concrete. Constr Build Mater 71:397–405
5. Duxson P, Fernández-Jiménez A, Provis JL, et al (2007) Geopolymer technology: The current state of the art. J Mater Sci 42:2917–2933. https://doi.org/10.1007/s10853-006-0637-z
6. Davidovits J (1994) Properties of Geopolymer Cements. In: First International Conference on Alkaline Cements and Concretes. Kiev State Technical University, Kiev, pp 131–149
7. Wu Y, Lu B, Bai T, et al (2019) Geopolymer, green alkali activated cementitious material: Synthesis, applications and challenges. Constr Build Mater 224:930–949. https://doi.org/10.1016/j.conbuildmat.2019.07.112
8. Farhan NA, Sheikh MN, Hadi MNS (2019) Investigation of engineering properties of normal and high strength fly ash based geopolymer and alkali-activated slag concrete compared to ordinary Portland cement concrete. Constr Build Mater 196:26–42. https://doi.org/10.1016/j.conbuildmat.2018.11.083
9. Phoo-Ngernkham T, Maegawa A, Mishima N, et al (2015) Effects of sodium hydroxide and sodium silicate solutions on compressive and shear bond strengths of FA-GBFS geopolymer. Constr Build Mater 91:1–8. https://doi.org/10.1016/j.conbuildmat.2015.05.001
10. Mayhoub OA, Mohsen A, Alharbi YR, et al (2021) Effect of curing regimes on chloride binding capacity of geopolymer. Ain Shams Eng J 12:3659–3668. https://doi.org/10.1016/j.asej.2021.04.032
11. Zhuang HJ, Zhang HY, Xu H (2017) Resistance of geopolymer mortar to acid and chloride attacks. Procedia Eng 210:126–131. https://doi.org/10.1016/j.proeng.2017.11.057
12. Pilehvar S, Szczotok AM, Rodríguez JF, et al (2019) Effect of freeze-thaw cycles on the mechanical behavior of geopolymer concrete and Portland cement concrete containing micro-encapsulated phase change materials. Constr Build Mater 200:94–103. https://doi.org/10.1016/j.conbuildmat.2018.12.057
13. Provis JL, Bernal SA (2014) Geopolymers and related alkali-activated materials. Annu Rev Mater Res 44:299–327. https://doi.org/10.1146/annurev-matsci-070813-113515
14. Ismail I, Bernal SA, Provis JL, et al (2014) Modification of phase evolution in alkali-activated blast furnace slag by the incorporation of fly ash. Cem Concr Compos 45:125–135. https://doi.org/10.1016/j.cemconcomp.2013.09.006
15. Dombrowski K, Buchwald A, Weil M (2007) The influence of calcium content on the structure and thermal performance of fly ash based geopolymers. J Mater Sci 42:3033–3043. https://doi.org/10.1007/s10853-006-0532-7
16. Yip CK, Van Deventer JSJ (2003) Microanalysis of calcium silicate hydrate gel formed within a geopolymeric binder. J Mater Sci 38:3851–3860
17. Wardhono A, Gunasekara C, Law DW, Setunge S (2017) Comparison of long term performance between alkali activated slag and fly ash geopolymer concretes. Constr Build Mater 143:272–279. https://doi.org/10.1016/j.conbuildmat.2017.03.153
18. Chen K, Wu D, Yi M, et al (2021) Mechanical and durability properties of metakaolin blended

with slag geopolymer mortars used for pavement repair. Constr Build Mater 281:. https://doi.org/10.1016/j.conbuildmat.2021.122566

19. Provis JL, Palomo A, Shi C (2015) Advances in understanding alkali-activated materials. Cem Concr Res 78:110–125

20. Cyr M, Pouhet R (2015) Resistance to alkali-aggregate reaction (AAR) of alkali-activated cement-based binders. In: Pacheco-Torgal F, Labrincha JA, Leonelli C, et al (eds) Handbook of Alkali-Activated Cements, Mortars and Concretes, 1st ed. Woodhead Publishing Limited, pp 397–422

21. Wang W, Noguchi T (2020) Alkali-silica reaction (ASR) in the alkali-activated cement (AAC) system : A state-of-the-art review. Constr Build Mater 252:

22. Krivenko P, Drochytka R, Gelevera A, Kavalerova E (2014) Mechanism of preventing the alkali-aggregate reaction in alkali activated cement concretes. Cem Concr Compos 45:157–165. https://doi.org/10.1016/j.cemconcomp.2013.10.003

23. Tänzer R, Jin Y, Dietmar S (2017) Effect of the inherent alkalis of alkali activated slag on the risk of alkali silica reaction. Cem Concr Res 98:82–90. https://doi.org/10.1016/j.cemconres.2017.04.009

24. Gifford P., Gillott JE (1996) Alkali-silica reaction (ASR) and alkali-carbonate reaction (ACR) in activated blast furnace slag cement (ABFSC) concrete. Cem Concr Res 26:21–26

25. Puertas F, Palacios M, Gil-Maroto A, Vázquez T (2009) Alkali-aggregate behaviour of alkali-activated slag mortars: Effect of aggregate type. Cem Concr Compos 31:277–284. https://doi.org/10.1016/j.cemconcomp.2009.02.008

26. Shi Z, Shi C, Zhao R, Wan S (2015) Comparison of alkali–silica reactions in alkali-activated slag and Portland cement mortars. Mater Struct Constr 48:743–751. https://doi.org/10.1617/s11527-015-0535-4

27. Lei J, Law WW, Yang EH (2021) Effect of calcium hydroxide on the alkali-silica reaction of alkali-activated slag mortars activated by sodium hydroxide. Constr Build Mater 272:. https://doi.org/10.1016/j.conbuildmat.2020.121868

28. Bakharev T, Sanjayan JG, Cheng YB (2001) Resistance of alkali-activated slag concrete to alkali–aggregate reaction. Cem Concr Res 31:331–334

29. Al-Otaibi S (2008) Durability of concrete incorporating GGBS activated by water-glass. Constr Build Mater 22:2059–2067. https://doi.org/10.1016/j.conbuildmat.2007.07.023

30. Fernández-Jiménez A, Puertas F (2002) The alkali-silica reaction in alkali-activated granulated slag mortars with reactive aggregate. Cem Concr Res 32:1019–1024. https://doi.org/10.1016/S0008-8846(01)00745-1

31. Xie Z, Xiang W, Xi Y (2003) ASR Potentials of Glass Aggregates in Water-Glass Activated Fly Ash and Portland Cement Mortars. J Mater Civ Eng 15:67–74. https://doi.org/10.1061/(asce)0899-1561(2003)15:1(67)

32. Li Z, Thomas RJ, Peethamparan S (2019) Alkali-silica reactivity of alkali-activated concrete subjected to ASTM C 1293 and 1567 alkali-silica reactivity tests. Cem Concr Res 123:. https://doi.org/10.1016/j.cemconres.2019.105796

33. Lindgård J, Andiç-Çakir Ö, Fernandes I, et al (2012) Alkali-silica reactions (ASR): Literature review on parameters influencing laboratory performance testing. Cem Concr Res 42:223–243. https://doi.org/10.1016/j.cemconres.2011.10.004

34. Rashidi M, Knapp MCL, Hashemi A, et al (2016) Detecting alkali-silica reaction : A multi-physics approach. Cem Concr Compos 73:123–135

35. Sanchez L (2014) Contribution to the assessment of damage in aging concrete infrastructures affected by alkali-aggregate reaction. Université de Laval

36. Sanchez LFM, Fournier B, Jolin M, et al (2017) Overall assessment of Alkali-Aggregate Reaction (AAR) in concretes presenting different strengths and incorporating a wide range of reactive aggregate types and natures. Cem Concr Res 93:17–31.

https://doi.org/10.1016/j.cemconres.2016.12.001

37. Fournier B, Bérubé M-A (2000) Alkali-aggregate reaction in concrete: a review of basic concepts and engineering implications. Can J Civ Eng 27:167–191. https://doi.org/10.1139/cjce-27-2-167

38. Smaoui N, Bérubé M-A, Fournier B, et al (2004) Evaluation of the expansion attained to date by concrete affected by alkali–silica reaction. Part I: Experimental study. Can J Civ Eng 31:826–845. https://doi.org/10.1139/l04-051

39. Sanchez LFM, Fournier B, Jolin M, Bastien J (2014) Evaluation of the stiffness damage test (SDT) as a tool for assessing damage in concrete due to ASR: Test loading and output responses for concretes incorporating fine or coarse reactive aggregates. Cem Concr Res 56:213–229. https://doi.org/10.1016/j.cemconres.2013.11.003

40. Sanchez LFM, Fournier B, Jolin M, Duchesne J (2015) Reliable quantification of AAR damage through assessment of the Damage Rating Index (DRI). Cem Concr Res 67:74–92. https://doi.org/10.1016/j.cemconres.2014.08.002

41. Sanchez LFM, Drimalas T, Fournier B, et al (2018) Comprehensive damage assessment in concrete affected by different internal swelling reaction (ISR) mechanisms. Cem Concr Res 107:284–303. https://doi.org/10.1016/j.cemconres.2018.02.017

42. Poyet S, Sellier A, Capra B, et al (2007) Chemical modelling of Alkali Silica reaction: Influence of the reactive aggregate size distribution. Mater Struct Constr 40:229–239. https://doi.org/10.1617/s11527-006-9139-3

43. Williamson T, Juenger MCG (2016) The role of activating solution concentration on alkali-silica reaction in alkali-activated fly ash concrete. Cem Concr Res 83:124–130. https://doi.org/10.1016/j.cemconres.2016.02.008

44. Singh J, Singh SP (2020) Evaluating the alkali-silica reaction in alkali-activated copper slag mortars. Constr Build Mater 253:. https://doi.org/10.1016/j.conbuildmat.2020.119189

45. Hajimohammadi A, van Deventer JSJ (2016) Dissolution behaviour of source materials for synthesis of geopolymer binders: A kinetic approach. Int J Miner Process 153:80–86. https://doi.org/10.1016/j.minpro.2016.05.014

46. Shi Z, Shi C, Wan S, Zhang Z (2017) Effects of alkali dosage and silicate modulus on alkali-silica reaction in alkali-activated slag mortars. Cem Concr Res 111:104–115. https://doi.org/10.1016/j.cemconres.2018.06.005

47. Yang C, Pu X (1999) Research on alkali-aggregate reaction of alkali-clinker-slag cement. J Chongqing Jianzhu Univ 21:14–19

48. Shi C, Shi Z, Hu X, et al (2015) A review on alkali-aggregate reactions in alkali-activated mortars/concretes made with alkali-reactive aggregates. Mater Struct Constr 48:621–628. https://doi.org/10.1617/s11527-014-0505-2

49. Shi Z, Shi C, Zhang J, et al (2018) Alkali-silica reaction in waterglass-activated slag mortars incorporating fly ash and metakaolin. Cem Concr Res 108:10–19. https://doi.org/10.1016/j.cemconres.2018.03.002

50. Khan MNN, Saha AK, Sarker PK (2021) Evaluation of the ASR of waste glass fine aggregate in alkali activated concrete by concrete prism tests. Constr Build Mater 266:. https://doi.org/10.1016/j.conbuildmat.2020.121121

51. Talling B, Brandstetr J (1989) Present state and future of alkali-activated slag concretes. ACI Spec Publ 114:1519–1546

52. Shi Z, Lothenbach B (2019) The role of calcium on the formation of alkali-silica reaction products. Cem Concr Res 126:. https://doi.org/10.1016/j.cemconres.2019.105898

53. Angulo-Ramírez DE, Mejía de Gutiérrez R, Medeiros M (2018) Alkali-activated Portland blast furnace slag cement mortars: Performance to alkali-aggregate reaction. Constr Build Mater 179:49–56. https://doi.org/10.1016/j.conbuildmat.2018.05.183

54. Hong SY, Glasser FP (2002) Alkali sorption by C-S-H and C-A-S-H gels: Part II. Role of alumina. Cem Concr Res 32:1101–1111. https://doi.org/10.1016/S0008-8846(02)00753-6

55. Hôpital EL, Lothenbach B, Saout G Le, et al (2015) Incorporation of aluminium in calcium-silicate-hydrates. Cem Concr Res 75:91–103

56. Rodrigue A, Duchesne J, Fournier B, et al (2020) Alkali-silica reaction in alkali-activated combined slag and fly ash concretes: The tempering effect of fly ash on expansion and cracking. Constr Build Mater 251:. https://doi.org/10.1016/j.conbuildmat.2020.118968

57. ASTM C1293-08b (2008) Standard test method for determination of length change of concrete due to alkali-silica reaction. Annu. B. ASTM Stand. 1–7

58. CAN/CSA-A23.2-14C-14 (2014) Obtaining and Testing Drilled Cores For Compressive Strength Testing

59. ASTM C1074-19e1 (2019) Standard Practice for Estimating Concrete Strength by the Maturity Method

60. Sanchez LFM, Fournier B, Jolin M, et al (2016) Use of Damage Rating Index to quantify alkali-silica reaction damage in concrete: Fine versus coarse aggregate. ACI Mater J 113:395–407. https://doi.org/10.14359/51688983

61. Sanchez LFM, Fournier B, Jolin M, Bastien J (2015) Evaluation of the Stiffness Damage Test (SDT) as a tool for assessing damage in concrete due to alkali-silica reaction (ASR): Input parameters and variability of the test responses. Constr Build Mater 77:20–32. https://doi.org/10.1016/j.conbuildmat.2014.11.071

62. Lawrence P, Cyr M, Ringot E (2003) Mineral admixtures in mortars. Cem Concr Res 33:1939–1947. https://doi.org/10.1016/S0008-8846(03)00183-2

63. Lothenbach B, Scrivener K, Hooton RD (2011) Supplementary cementitious materials. Cem Concr Res 41:1244–1256. https://doi.org/10.1016/j.cemconres.2010.12.001

64. Saha AK, Khan MNN, Sarker PK, et al (2018) The ASR mechanism of reactive aggregates in concrete and its mitigation by fly ash: A critical review. Constr Build Mater 171:743–758. https://doi.org/10.1016/j.conbuildmat.2018.03.183

65. Thomas M (2011) The effect of supplementary cementing materials on alkali-silica reaction: A review. Cem Concr Res 41:1224–1231. https://doi.org/10.1016/j.cemconres.2010.11.003

66. Lee NK, Jang JG, Lee HK (2014) Shrinkage characteristics of alkali-activated fly ash/slag paste and mortar at early ages. Cem Concr Compos 53:239–248. https://doi.org/10.1016/j.cemconcomp.2014.07.007

67. Chi M, Huang R (2013) Binding mechanism and properties of alkali-activated fly ash/slag mortars. Constr Build Mater 40:291–298. https://doi.org/10.1016/j.conbuildmat.2012.11.003

68. Hossain MM, Karim MR, A Elahi MM, Mohd Zain MF (2020) Water absorption and sorptivity of alkali-activated ternary blended composite binder. J Build Eng 31:101370. https://doi.org/10.1016/j.jobe.2020.101370

69. Chithiraputhiran S, Neithalath N (2013) Isothermal reaction kinetics and temperature dependence of alkali activation of slag, fly ash and their blends. Constr Build Mater 45:233–242. https://doi.org/10.1016/j.conbuildmat.2013.03.061

70. Sanchez LFM, Fournier B, Jolin M, et al (2017) Tools for assessing damage in concrete affected by AAR coming from fine and coarse aggregates. Rev IBRACON Estruturas e Mater 10:84–91. https://doi.org/10.1590/s1983-41952017000100005

71. Sanchez LFM, Fournier B, Jolin M, et al (2016) Practical use of the Stiffness Damage Test (SDT) for assessing damage in concrete infrastructure affected by alkali-silica reaction. Constr Build Mater 125:1178–1188. https://doi.org/10.1016/j.conbuildmat.2016.08.101

72. Rangan B V. (2009) Engineering properties of geopolymer concrete. In: Provis JL, van Deventer JSJ (eds) Geopolymers: Structures, Processing, Properties and Industrial Applications, 1st ed. Woodhead Publishing Limited, pp 211–226